Effects of Microdomain Structures on the Molecular Orientation of Poly(styrene-*block*-butadiene-*block*-styrene) Triblock Copolymer

Shinichi Sakurai,* June Sakamoto, Mitsuhiro Shibayama, and Shunji Nomura

Department of Polymer Science and Engineering, Kyoto Institute of Technology, Matsugasaki, Kyoto 606, Japan

Received December 1, 1992; Revised Manuscript Received March 16, 1993

ABSTRACT: Effects of microdomain structures on the molecular orientation of poly(styrene-*block*-butadiene-*block*-styrene) triblock copolymer (SBS) were investigated. The microdomain morphology was controlled by changing a casting solvent when the specimen was cast from a solution. Polystyrene (PS)–polybutadiene (PB) alternating lamellar, PB-cylindrical, and PS–PB bicontinuous microdomain structures were obtained by using toluene, methyl ethyl ketone (MEK), and heptane, respectively. The molecular orientation behavior for PS and PB chains with the uniaxial strain turned out to depend on the morphology of undrawn films and to have a correlation with the stress–strain behavior. It was also found that values of dichroic orientation factor F_D of the absorption bands at 1493 and 966 cm^{-1} for PS and PB chains, respectively, are negative irrespective of morphologies and strains. From the microscopic (molecular orientation) and macroscopic (stress–strain behavior) studies, changes in the microdomain structures were considered in relation to the morphology of the undrawn specimen.

I. Introduction

Multicomponent polymeric systems have been studied for more than 20 years so as to develop new types of materials having various functions and properties.[1–22] Block copolymers in the microphase-separated state are good examples to study the structure–property relationship in multicomponent systems. Since the mechanical properties depend on the morphology of the block copolymers, the deformation mechanism of the microdomain structures has been intensively studied by small-angle X-ray scattering and electron microscopy.[4–7,10–13,18] Recently, infrared spectroscopy (IR) has been applied for the structural study of the multiphase polymer systems.[15,16,21,22] IR is of a great advantage in studies of the multicomponent system because it is possible to analyze separately the behavior of infrared absorption bands of interest. Since the orientation behavior with the strain is closely related to changes in microdomain structures, the studies of the molecular orientation by IR can be applied for the investigations of the deformation mechanism of the structures.

The IR studies on poly(styrene-*block*-butadiene-*block*-styrene) triblock copolymer (SBS) have been already presented in the 1970s.[2,3,14] Recently, the IR technique was successfully applied by Zhao[22] for the study of structural relaxation in the stretched SBS with cylindrical microdomains of polystyrene (PS). He was probably the first to discuss the molecular orientation in terms of the structural changes with the strain or annealing. However, only the polybutadiene (PB) orientation was investigated. In fact, in most cases of the studies on the orientation for block copolymers, only the orientation of PB chains was discussed and that of PS chains was seldom done. This is mainly due to the difficulty in detecting the orientation of PS chains. However, more recently, Noda et al.[15,16] found the orientation of PS chains in the block copolymers by means of dynamic infrared linear dichroism (DIR) with a very small periodical strain.

In our study, the molecular orientations for both PS and PB chains in the presence of the microdomains were successfully analyzed and the effects of microdomain structures on the molecular orientation with the uniaxial strain were investigated. The absorption bands for PS and PB, which are sensitive to the molecular orientation, were identified based on the number of infrared dichroism studies on SBS,[2,3,14–16,22] PS,[23–26] and PB.[27] The morphology was controlled by changing a casting solvent when the specimen was cast from a solution.[1,2,11,20] PS–PB alternating lamellae, PB–cylinders in a PS matrix, and PS–PB bicontinuous microdomain structures were obtained by using toluene, methyl ethyl ketone (MEK), and heptane, respectively. Since the orientation behavior with the strain is closely related to the structure, we can discuss the deformation mechanisms of microdomain structures for the three types of morphology.

II. Experimental Section

The SBS specimen, TR2400 (Japan Synthetic Rubber Co., Ltd.), used in this study has a number-average molecular weight (M_n) of 6.31×10^4, a heterogeneity index for molecular weight (M_w/M_n) of 1.15, where M_w denotes the weight-average molecular weight, and a weight fraction of PS (w_{PS}) of 0.56. The microstructures of PB chains are 33, 55, and 12 wt % of cis-1,4-, trans-1,4-, and 1,2-linkages, respectively. More details in the characterization are described elsewhere.[20] The SBS specimen was dissolved in a solvent to prepare approximately a 5 wt % polymer solution. Film samples were obtained by evaporating gradually the solvent at room temperature.

The morphology in an as-cast specimen can be changed with the selectivity of the cast solvent for SBS triblock copolymers.[1,2,11,20] In this study, three kinds of solvent were used, i.e., toluene, methyl ethyl ketone (MEK), and a heptane/methylene chloride (1/1) mixture. Methylene chloride in the solvent mixture was used to obtain a homogeneous heptane solution of TR2400 because it was impossible to dissolve the specimen directly in pure heptane. Since the boiling temperature of methylene chloride (40 °C) is much lower than that of heptane (98 °C), the SBS solution in the heptane/methylene chloride (1/1) mixture would become a homogeneous heptane solution in an early stage of casting. Here, the homogeneous solution means the solution in which the concentration of the copolymer is constant everywhere. It is needless to say that the concentration may be fluctuating in a microscopic scale due to micelle formation in the block copolymer solution. The values of the solubility parameter[28] for PS, PB, and these solvents are tabulated in Table I. Since

* To whom correspondence should be addressed.

0024-9297/93/2226-3351$04.00/0

Table I. Solubility Parameter Values for Three Kinds of Casting Solvent and PS and PB, Solvent Selectivity, and the Morphology Revealed by TEM

casting solvent	solubility param $(cal/cm^3)^{1/2}$	solvent selectivity	morphology
toluene	8.9	neutral	lamellae
MEK	9.3	selective to PS	PB cylinders
heptane	7.4	selective to PB	PS–PB bicontinuous microdomains
H/MC[a] (1/1)	~8.6[b]	neutral[c]	
PS	8.6–9.7		
PB	8.1–8.6		

[a] Heptane/methylene chloride mixture. [b] This value was estimated from the values of the solubility parameter of 7.4 and 9.7 $(cal/cm^3)^{1/2}$ for heptane and methylene chloride, respectively. [c] The heptane/methylene chloride (1/1) mixture is neutral for SBS, assuming no phase separation of the solvent mixture due to the difference in selectivity of the individual solvent molecule to PS and PB.

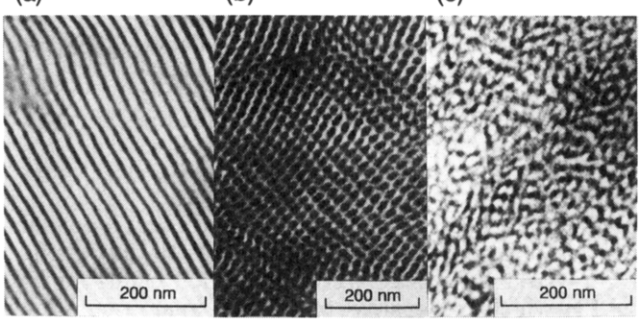

Figure 1. Transmission electron micrographs of the ultrathin sections of TR2400 stained with osmium tetroxide (OsO_4): (a) toluene as-cast film; (b) MEK as-cast film; (c) heptane as-cast film.

the solvent whose value is closer to that for a polymer can dissolve the polymer better, toluene is a neutral solvent, MEK is a selectively good solvent for PS, and heptane is a selectively good solvent for PB. Thickness was in the range of 30–40 μm for the toluene as-cast films, 60–70 μm for the MEK as-cast films, and 50–60 μm for the heptane as-cast films.

For tensile stress–strain measurements, CATY-500BH (Yonekura Co., Ltd.) was used with a rectangular-shaped film specimen of 10-mm width, which was cramped between a pair of chucks 30-mm apart from each other. The drawing speed was 50 mm/min. Note that the stress shown in Figures 5–7 is the nominal stress, which is the drawing force divided by the cross-sectional area of the undrawn film. The stretching direction (SD) is parallel to the surface of the as-cast films (see Figure 2). Infrared spectrograms were obtained at every increment of 25% strain using a FIRIS 100 FTIR (Fourier transform infrared) spectrometer (Fuji Electric Co., Ltd.) operating at a number of scans of 64 and a spectral resolution of 4 cm^{-1}. Since the actual FTIR spectrum is comprised of several individual absorption peaks overlapping each other, the spectrum should be decomposed into individual contributions in order to evaluate accurate values of a dichroic ratio. The peak decomposition was performed with a peak-resolving software developed in our laboratory,[29] where the individual peak is assumed to be represented by a weighted sum of Gaussian and Lorentzian functions. The tensile stress–strain measurements and the FTIR measurements were done at room temperature.

III. Results

Transmission electron microscopy (TEM) was conducted in order to survey the morphologies in the as-cast specimens. TEM results are presented in Figure 1 where the dark regions correspond to the PB microdomains stained with osmium tetroxide (OsO_4) and the bright regions to the PS microdomains. In the toluene as-cast specimen a lamellar morphology can be seen, which is a

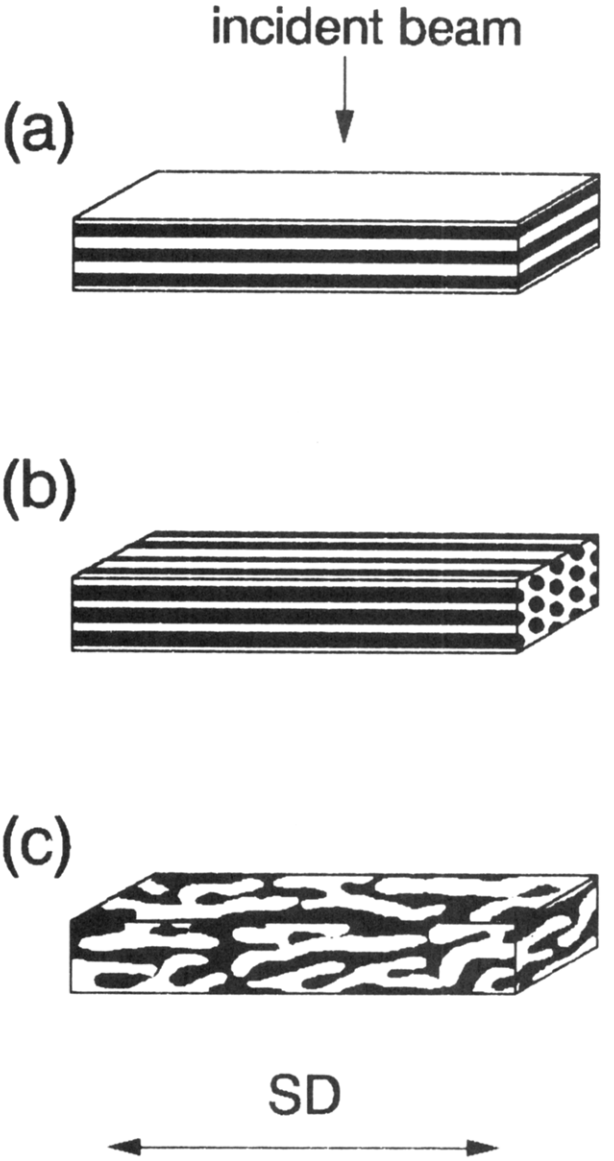

Figure 2. Schematic representation showing the relationship between the orientation of the microdomains and the stretching direction (SD), with PS and PB microdomains shown in white and black, respectively: (a) toluene as-cast film; (b) MEK as-cast film; (c) heptane as-cast film. Note that for the MEK as-cast film the overall orientation of the cylinder axes is random within the plane parallel to the film surface, although a single crystal of the PB cylinders is displayed in part b for simplicity.

thermodynamically equilibrium morphology for this SBS specimen with $w_{PS} = 0.56$.[20] Hexagonally packed PB cylinders in the PS matrix and PS–PB bicontinuous microdomain structures were observed in the MEK as-cast and heptane as-cast specimens, respectively.

Figure 2 schematically shows the relationship between the orientation of the microdomains and the stretching direction (SD), with PS and PB microdomains shown in white and black, respectively. For the toluene as-cast film, SD is approximately parallel to the lamellar microdomains as presented in part a since the lamellae were preferentially formed parallel to the surface of the as-cast film.[8,9] In part b the case of the MEK as-cast film is shown. SD is parallel to the plane in which the axes of PB cylinders are preferentially oriented, since such a plane was found to be parallel to the surface of the as-cast film.[20] Note that the overall orientation of the cylinder axes is random in this plane, although a single crystal of the PB cylinders is displayed in part b for simplicity. Contrary to the

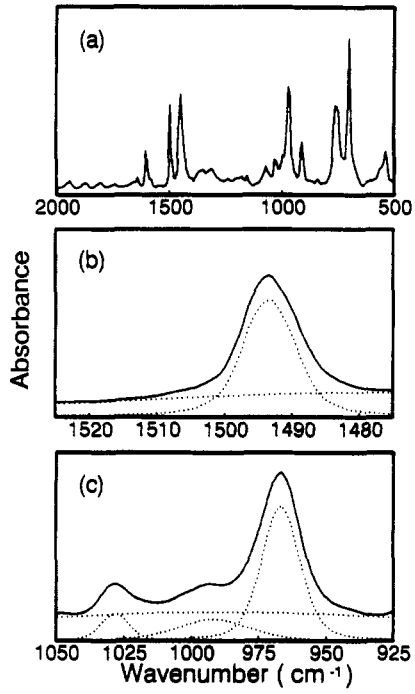

Figure 3. Infrared absorption spectrum of a toluene as-cast film of TR2400 at room temperature at wavenumbers from 500 to 2000 cm^{-1} in part a. The decomposed spectra (dotted lines) with the original spectra (solid lines) at wavenumbers from 1475 to 1525 cm^{-1} in part b and those at wavenumbers from 925 to 1050 cm^{-1} in part c.

toluene and MEK as-cast films, no preferential orientation of PS–PB bicontinuous microdomains may be considered for the heptane as-cast film and hence the scheme is as depicted in part c.

In order to evaluate the molecular orientation separately for PS and PB, the absorption bands which are sensitive to the respective orientation are required. These bands can be identified based on a number of infrared dichroism studies on SBS,[2,3,14-16,22] PS,[23-26] and PB.[27] The band at 1493 cm^{-1} turned out to the best for PS since there is no specific absorption due to PB in the vicinity of this band. The band is assigned to a phenyl ring deformation mode in the direction parallel to the C–C bond between the main chain and a phenyl ring. This vibrational mode for PS is generally recognized to be perpendicular to the axis of the chain segment.[3,23,26] For evaluation of the molecular orientation of PB chains, the absorption band located at 966 cm^{-1}, which is ascribed to an out-of-plane CH bending mode in *trans*-1,4-butadiene, was used. This band was shown by many authors[14-16,27] to be sensitive to orientation, and a transition moment for the vibration was also observed to be roughly perpendicular to the axis of the chain segment.

An infrared absorption spectrum of a toluene as-cast film of TR2400 at room temperature is shown in Figure 3a at wavenumbers from 500 to 2000 cm^{-1}. The dichroic ratio D is given as:

$$D = A_{\parallel}/A_{\perp} \tag{1}$$

where $A_{\parallel}$ and $A_{\perp}$ denote the absorbances of light polarized parallel and perpendicular to SD of the specimen, respectively. The peak area of the decomposed individual contribution for the absorption band was used to calculate the D values. The decomposed spectra are shown with the original spectra at wavenumbers from 1475 to 1525 cm^{-1} in Figure 3b and at wavenumbers from 925 to 1050 cm^{-1} in Figure 3c. The molecular orientation can be discussed quantitatively by means of the orientation factor

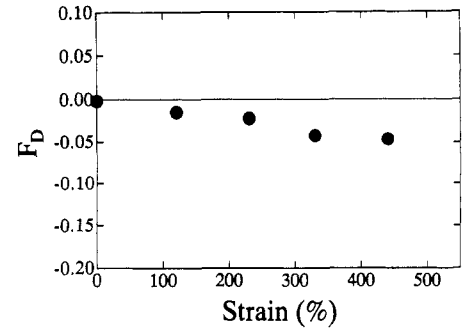

Figure 4. Dichroic orientation factor F_D as a function of the strain for the drawn atactic polystyrene films, which were evaluated from the dichroic ratio D for the absorption band at 1493 cm^{-1}. The PS films were drawn by 2.2, 3.3, 4.3, and 5.4 draw ratios at 110 °C and were quenched instantaneously to room temperature.

f which is defined as:

$$f = (1/2)(3\langle\cos^2\theta\rangle - 1) \tag{2}$$

where θ is the angle between SD and the axis of the chain segment. f is related to the dichroic ratio D of a given absorption band by:

$$f = \frac{D_0 + 2}{D_0 - 1}\frac{D - 1}{D + 2} \tag{3}$$

Here D_0 is given by

$$D_0 = 2\cot^2\alpha \tag{4}$$

where α is the angle between the axis of the chain segment and the transition moment contributing to the absorption under consideration. Generally it is not easy to evaluate α accurately and hence to evaluate f. Instead, the quantity $(D-1)/(D+2)$ which is proportional to f is satisfactory for our purpose because only the qualitative changes in the molecular orientation with the uniaxial strain are discussed in this study. The quantity is referred to as the dichroic orientation factor F_D; i.e.

$$F_D = \frac{D - 1}{D + 2} \tag{5}$$

Since the PS band at 1493 cm^{-1} was considered to be insensitive to orientation,[14] i.e., $\alpha \cong 54.74°$ which causes $F_D = 0$ irrespective of the orientation factor f,[30] we examine this absorption band using drawn films of homopolystyrene. The atactic polystyrene provided from the Idemitsu Petrochemical Co., Ltd. (sample code HH30E), was used. $M_w = 2.6 \times 10^5$ and $M_w/M_n = 2.7$ for this specimen. The PS films were drawn to 2.2, 3.3, 4.3, and 5.4 draw ratios at 110 °C and were quenched instantaneously to room temperature. As presented in Figure 4, F_D evaluated from the dichroic ratio D for the band at 1493 cm^{-1} shows negative values with the strain, although the absolute values are smaller than those for PB shown in Figures 5–7. Thus, it is confirmed that the PS absorption band at 1493 cm^{-1} can be utilized for the evaluation of the molecular orientation with noting the negative orientation of this transition moment.

Before discussing the morphology dependence of the stress–strain and the molecular orientation behavior, we discuss briefly the experimental observations generally seen for all specimens. Necking of the specimens was observed from an initial stage of the strain, indicating that the specimens suffered the plastic deformation. The stress increased drastically in a very early stage of the strain, which was followed by a bit of the stress relaxation and became roughly constant in the successive strain. The

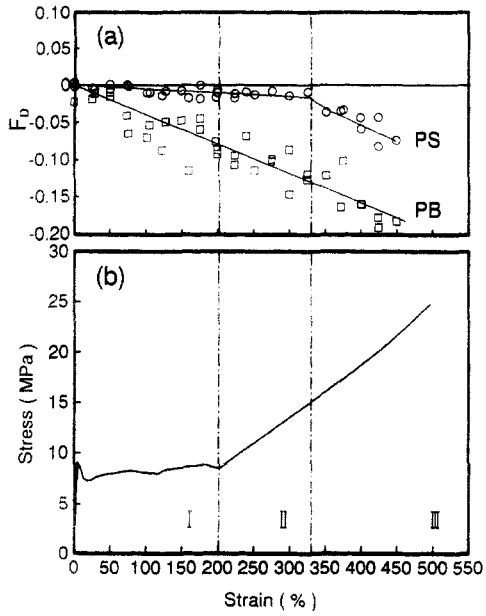

Figure 5. Dichroic orientation factor F_D for PS and PB chains as a function of the strain in part a and the stress–strain behavior in part b for the toluene as-cast film. Note that SD is approximately parallel to the lamellar microdomains.

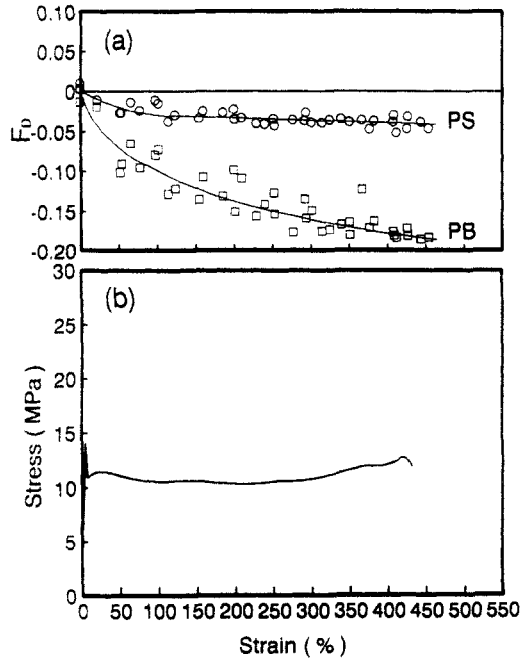

Figure 6. Dichroic orientation factor F_D for PS and PB chains as a function of the strain in part a and the stress–strain behavior in part b for the MEK as-cast film. SD is parallel to the plane in which the axes of PB cylinders are preferentially oriented.

values of the dichroic orientation factor F_D for both PS and PB are negative, irrespective of the morphologies and strains, which were evaluated from the dichroic ratios for the absorption bands at 1493 and 966 cm^{-1} for PS and PB chains, respectively.

Figure 5 shows the dichroic orientation factor F_D for PS and PB chains as a function of the strain in part a and the stress–strain behavior in part b for the toluene as-cast film. Recall that SD is approximately parallel to the lamellar microdomains. We discuss the stress–strain behavior and the molecular orientation by dividing these behaviors into three regions. In region I from 0 to 200% strain, gradual orientation of PS chains and pronounced orientation of PB chains can be seen with the strain. Region II is from 200 to 330% strain where the continuous

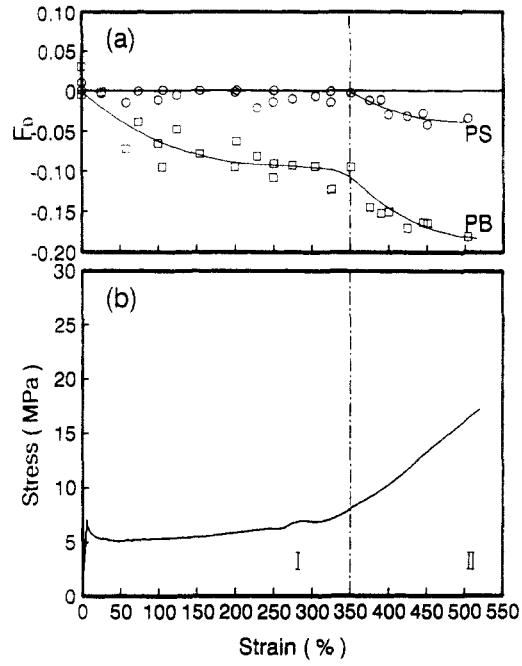

Figure 7. Dichroic orientation factor F_D for PS and PB chains as a function of the strain in part a and the stress–strain behavior in part b for the heptane as-cast film. Note that the morphology revealed by TEM is PS–PB bicontinuous microdomains.

orientations of PS and PB chains were observed. An increase in the stress with the strain can be detected, which is relevant to the so-called strain-induced plastic-to-rubber transition.[4-7] In the final region III from 330% strain up to break, the stress continued to increase. The characteristic finding in this region is a drastic progress in the orientation of PS chains, whereas the orientation of PB chains showed a slight change with the strain.

Figure 6 shows the dichroic orientation factor F_D for PS and PB chains as a function of the strain in part a and the stress–strain behavior in part b for the MEK as-cast film. SD is parallel to the plane in which the axes of PB cylinders are preferentially oriented. The orientation of PB chains monotonically proceeded with the strain up to break. PS chains were gradually oriented until ca. 120% strain and showed no remarkable change afterward. The stress at the yielding point is larger than that of the toluene as-cast film and was roughly constant until break. Thus, the stress–strain behavior showed only plastic deformation without the plastic-to-rubber transition, opposite to the toluene as-cast film. One can see similarities in both the molecular orientation and the stress–strain behavior between the MEK as-cast film and the toluene as-cast film in its region I. Again this indicates that the behavior of the MEK as-cast film was not followed by such rubbery behavior as observed in regions II and III of the toluene as-cast film. Such behavior for the MEK as-cast film is related to the morphology of the undrawn specimen in which the matrix phase is composed of the glassy PS phase.

Figure 7 shows the dichroic orientation factor F_D for PS and PB chains as a function of the strain in part a and the stress–strain behavior in part b for the heptane as-cast film. The morphology revealed by TEM is PS–PB bicontinuous microdomain structures. The significant change in the molecular orientation for both PS and PB chains occurred at 350% strain which corresponds to the onset of an increase in the stress, so the behavior can be divided into two regions. Then one can recognize similar behavior of regions I (0–350% strain) and II (350% strain to break) with those of regions I and II/III of the toluene as-cast film, respectively. The stress at the yielding point

was the smallest among the three kinds of specimens. The lowest energy required for the plastic deformation is ascribed to less connectivity of the glassy PS microdomains in the heptane as-cast film compared to the other two kinds of specimens. In fact, the behaviors of the stress–strain and molecular orientation were very similar to those obtained for the different SBS with PS-cylindrical microdomains,[21] except for the larger yielding stress and obvious orientation of PS chains for the heptane as-cast film of TR2400.

IV. Discussion

It was found that the evaluated values of F_D for the PS absorption band at 1493 cm^{-1} were negative, as presented in Figure 4. Thus, the sensitivity of this absorption band to orientation was clearly confirmed, and the phenyl rings can be considered to be oriented perpendicular to SD. The negative orientation for the 1493-cm^{-1} band is consistent with the results reported previously.[3,23,26] However, Noda et al.[16] reported parallel orientation of the phenyl rings to SD at 30 °C. The oriented films of syndiotactic PS with a draw ratio of 4 were used in the former case,[26] and a very small strain, i.e., ca. 0.1%, in the oscillatory tensile strain for DIR measurements was applied in the latter case.[16] Although discrepancy on the orientation of the phenyl rings at 30 °C may lie in how much strain was applied, it is beyond the scope of this study to make further discusson. In the following discussion, it is considered that the negative value of F_D for the 1493-cm^{-1} band indicates the parallel orientation of PS chains to SD. As for the PB absorption band at 966 cm^{-1}, the direction of a transition moment is roughly perpendicular to the axis of the chain segment and hence it is also considered that the negative value of F_D indicates the parallel orientation of PB chains to SD.

We now construct approximate schemes for the structural change involved in the uniaxial strain from the microscopic (molecular orientation) and macroscopic (stress–strain behavior) studies. First of all, the following fact should be noticed at this stage: For an undrawn specimen, the orientations of the block chains in the microdomains were shown to be trivial in spite of a strong constraint of the localization of the chemical junctions of PS and PB blocks.[31] Therefore, detectable orientation for PS chains in the glassy state is ascribed not to the deformation or orientation of PS microdomains but to PS fibrils. The models for the structural deformation are presented in Figure 8 for (a) toluene, (b) MEK, and (c) heptane as-cast films, where the glassy PS domains and the rubbery PB domains are shown in white and black, respectively. For the toluene as-cast film, micronecking in the glassy PS lamellae first occurred, and PS and PB chains were stretched parallel to SD. From the beginning of region I, PB chains were effectively stretched because the glassy fractured PS microdomains which were dispersed in the rubbery matrix played as physical crosslinks with accompanying deformation of the PS microdomains themselves. Under the successive stretching in region II the orientation of PS chains proceeded, indicating that the PS microdomains were gradually segmented into smaller domains involved in the orientation of PB chains. In region III, PS chains showed remarkable change in the orientation behavior while PB chains showed a slight change. It may be expected that PB chains already reached an extremely stretched state and that the PS microdomains are highly deformed, and in consequence the stress increased with the strain.

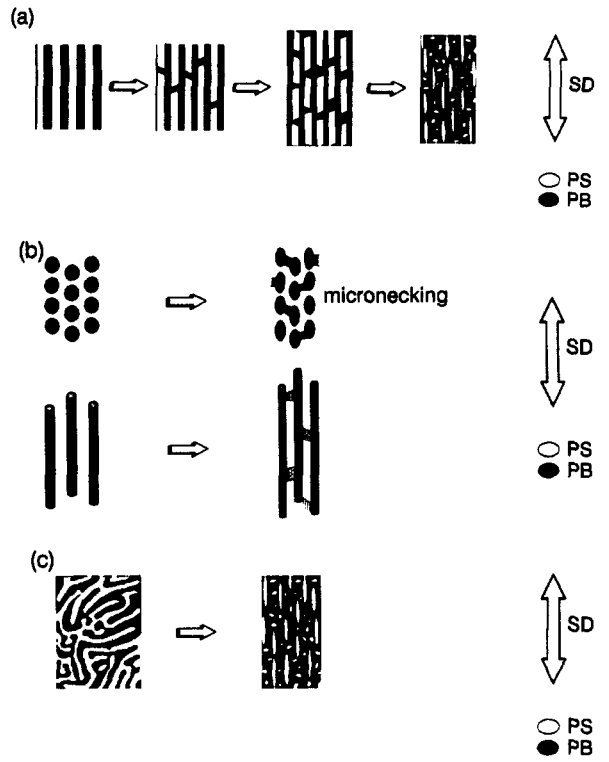

Figure 8. Schemes for the structural change involved in the uniaxial strain. The models are presented for (a) toluene, (b) MEK, and (c) heptane as-cast films, where the glassy PS domains and the rubbery PB domains are shown in white and black, respectively.

For the MEK as-cast film, continuous orientation of both PS and PB chains with the strain and no strain-induced plastic-to-rubber transition was seen in the entire region from 0% strain up to break. This is because the matrix is composed of the glassy PS phase, as stated above. From an initial stage of the strain, the glassy PS matrix is necessarily deformed to some extent along with necking. As schematically shown in Figure 8b, the necking does not instantaneously proceed over the specimen because of the presence of the PB-cylindrical microdomains and hence the necking can be localized. Before fragmentation of the glassy PS matrix and dispersion of resultant fragmentary PS microdomains into the rubbery PB phase, the micronecking grows macroscopically and the specimen breaks.

The structural change for the heptane as-cast film may be similar to that for the toluene as-cast film, as schematically presented in Figure 8c. It is expected that the continuous strut of glassy PS microdomains in the heptane as-cast film is easier to break than PS lamellae in the toluene as-cast film and that as-fractured PS microdomains may be smaller than those existing in region I of the toluene as-cast film. Moreover, the structure in the undrawn heptane as-cast film is flexibly considered to be similar to the fractured lamellar structure in region I or II for the toluene as-cast film. Therefore, the level of the stress at break is anticipated to be similar. However, it was smaller for the heptane as-cast film than for the toluene as-cast film. This may be ascribed to the extent of PB microdomains in undrawn specimens. The continuous strut of the PB microdomains in the heptane as-cast film is not as strong against the stress as the lamellar PB microdomains in the toluene as-cast film. The schemes for the structural changes presented here are in good agreement with the results by TEM on the lamellar[4–7,12] and cylindrical[7,10,13] morphologies.

V. Conclusion

Molecular orientation behavior with uniaxial strain for PS and PB chains turned out to depend on morphology of an undrawn film and to have a strong correlation with the stress–strain behavior. It was also found that the values of the dichroic orientation factor F_D, which were evaluated from the dichroic ratios for the absorption bands at 1493 and 966 cm^{-1} for PS and PB chains, respectively, were negative irrespective of morphologies and strains. From the microscopic (molecular orientation) and macroscopic (stress–strain behavior) studies, changes in microdomain structures were considered in relation to the morphology of an undrawn film. For the toluene as-cast film, there were three regions among which the orientation and mechanical behaviors with the strain differ substantially. Micronecking in PS lamellae and the stretching of PB chains parallel to SD, which were accompanied by the strain-induced plastic-to-rubber transition, can be considered in region I, the higher orientation of PB chains in region II, and the extremely stretched PB chains with remarkable deformation of further segmented PS microdomains in region III. For the MEK as-cast film, continuous orientation of both PS and PB chains with the strain and no strain-induced plastic-to-rubber transition was seen in the entire region from 0% strain up to break, since the matrix is composed of the glassy PS phase. By the existence of rubbery PB microdomains in the glassy PS matrix, the necking in the PS matrix does not instantaneously proceed and hence the necking can be localized. Before fragmentation of the glassy PS matrix and dispersion of resultant fragmentary PS microdomains into the PB phase, the necking grows macroscopically and the specimen breaks. As for the heptane as-cast film, the structural change is considered to be similar to that of the fractured lamellar structure for the toluene as-cast film.

Acknowledgment. The authors are grateful to Dr. T. Takebe at the Idemitsu Petrochemical Co., Ltd., for kindly providing the drawn films of the atactic polystyrene, HH30E.

References and Notes

(1) Wilkes, G. L.; Stein, R. S. *J. Polym. Sci.* **1969**, *A2*, 1525.
(2) Read, B.; Wilkes, G. L.; Stein, R. S., unpublished results.
(3) Folkes, M. J.; Keller, A. *J. Polym. Sci., Polym. Phys. Ed.* **1976**, *14*, 833.
(4) Fujimura, M.; Hashimoto, T.; Kawai, H. *Rubber Chem. Technol.* **1978**, *51*, 215.
(5) Kawai, H.; Hashimoto, T. In *Contemporary Topics in Polymer Science*; Shen, M., Ed.; Plenum Press: New York, 1979; Vol. 3, p 245.
(6) Hashimoto, T.; Fujimura, M.; Saijo, K.; Kawai, H.; Diamant, J.; Shen, M. In *Multiphase Polymers*; Cooper, S. L., Estes, G. M., Eds.; Advances in Chemistry Series 176; American Chemical Society: Washington, DC, 1979; p 257.
(7) Kawai, H.; Hashimoto, T.; Miyoshi, K.; Uno, H.; Fujimura, M. *J. Macromol. Sci., Phys.* **1980**, *B17* (3), 427.
(8) Hashimoto, T.; Shibayama, M.; Kawai, H. *Macromolecules* **1980**, *13*, 1237.
(9) Hashimoto, T.; Tanaka, H.; Hasegawa, H. *Macromolecules* **1985**, *18*, 1864.
(10) Pakula, T.; Saijo, K.; Kawai, H.; Hashimoto, T. *Macromolecules* **1985**, *18*, 1294.
(11) Séguéla, R.; Prud'homme, J. *Macromolecules* **1978**, *11*, 1007.
(12) Séguéla, R.; Prud'homme, J. *Macromolecules* **1981**, *14*, 197.
(13) Séguéla, R.; Prud'homme, J. *Macromolecules* **1988**, *21*, 635.
(14) Kraus, G.; Rollmann, K. W. *J. Macromol. Sci., Phys.* **1980**, *B17* (3), 407.
(15) Noda, I.; Dowrey, A. E.; Marcott, C. In *Fourier Transform Infrared Characterization of Polymers*; Ishida, H., Ed.; Plenum Publishing Corp.: New York, 1987; pp 33–59.
(16) Noda, I.; Smith, S. D.; Dowrey, A. E.; Grothaus, J. T.; Marcott, C. *Mater. Res. Soc. Symp. Proc.* **1990**, *171*, 117.
(17) Matsushita, Y.; Nakao, Y.; Saguchi, R.; Mori, K.; Choshi, H.; Muroga, Y.; Noda, I.; Nagasawa, M.; Chang, T.; Glinka, C. J.; Han, C. C. *Macromolecules* **1988**, *21*, 1802.
(18) Polizzi, S.; Bösecke, P.; Stribeck, N.; Zachmann, H. G.; Zietz, R.; Bordeianu, R. *Polymer* **1990**, *31*, 638.
(19) Sakurai, S.; Okamoto, S.; Kawamura, T.; Hashimoto, T. *J. Appl. Crystallogr.* **1991**, *24*, 679.
(20) Sakurai, S.; Momii, T.; Taie, K.; Shibayama, M.; Nomura, S.; Hashimoto, T. *Macromolecules* **1993**, *26*, 485.
(21) Sakamoto, J.; Sakurai, S.; Doi, K.; Nomura, S., submitted for publication in *Polymer*.
(22) Zhao, Y. *Macromolecules* **1992**, *25*, 4705.
(23) Painter, P. C.; Koenig, S. L. *J. Polym. Sci., Polym. Phys. Ed.* **1977**, *15*, 1885.
(24) Noda, I. *J. Am. Chem. Soc.* **1989**, *111*, 8116.
(25) Noda, I. *Appl. Spectrosc.* **1990**, *44*, 550.
(26) Reynolds, N. M.; Hsu, S. L. *Macromolecules* **1990**, *23*, 3463.
(27) Hsu, S. L.; Moore, W. H.; Krimm, S. *J. Appl. Phys.* **1975**, *46*, 4185.
(28) Grulke, E. A. In *Polymer Handbook*, 3rd ed.; Brandrup, J., Immergut, E. H., Eds.; Wiley: New York, 1989.
(29) Yamamoto, T.; Shibayama, M.; Nomura, S. *Polym. J.* **1989**, *11*, 895.
(30) From eq 3 one gets $F_D = f[(D_0 - 1)/(D_0 + 2)]$. Since $\alpha \simeq 54.74°$ gives $D_0 = 1$, hence $F_D = 0$, irrespective of the value of f.
(31) Shibayama, M.; Hashimoto, T.; Meier, D. J. *Macromolecules* **1985**, *18*, 1855.